ORIGINAL PAPER

Sulphuric acid-functionalized siliceous zirconia as an efficient and reusable catalyst for the synthesis of glycerol triacetate

Km Abida[1] · Amjad Ali[1]

Abstract

In the present study, a sulphated siliceous zirconia catalyst (SSZ-550) has been prepared and characterized by XRD and FTIR analysis to indicate the incorporation of sulphate group over the matrix. X-ray photoelectron spectroscopy also revealed that sulphur group was incorporated over the matrix to impart the Brønsted acidity to the catalyst which is vital for the acetylation activity. To optimize the reaction parameters, viz. reagent molar ratios (3–12; glycerol/acetic acid), catalyst amount (1–5 wt%; catalyst/glycerol), reaction duration (20–50 min) and reaction temperature (30–100 °C) have been varied to obtain the optimum catalyst activity for the maximum glycerol triacetate yield. Finally, under the optimized reaction parameters of 9:1 glycerol/acetic acid molar ratio, 3 wt% catalyst, 80 °C reaction temperature and 40 min of reaction duration, a 93% glycerol triacetate yield was obtained. The catalyst was recovered from the reaction mixture and reused during six consecutive reaction runs while retaining 50% glycerol triacetate selectivity in the last cycle. A plausible mechanism suggests the heterogeneous catalyst-assisted protonation of carbonyl group of acetic acid to initiate the stepwise esterification of the hydroxyl groups of glycerol.

Keywords Glycerol · Glycerol triacetate · Acetic acid · HPLC

Introduction

The demand and cost of the biodiesel (BD) have been constantly increased over the past few years (Edward et al. 2014). The production of global BD is expected to reach almost 39 billion litres by 2024, and accordingly the glycerol (GL) production, a by-product from BD industry, is bound to increase many fold (FAO, OECD 2015; Khadijeh et al. 2014). GL is considered as a nontoxic molecule having a variety of application in the synthesis of monoglyceride, diglyceride (Fregolente et al. 2010), glycerol carbonate (Jiahui et al. 2018), glycerol monoacetate (GM), glycerol diacetate (GD) and glycerol triacetate (GT) (Malaika and Kozłowski 2018). GT is an important derivative of GL

having a variety of applications in pharmaceuticals, fuel, cosmetic and food industry (Goscianska and Malaika 2019). As a bio-additive, GD and GT could be utilized to enhance the cold flow properties and to improve the viscosity of the BD fuel (Malaika and Kozłowski 2018). These molecules have also been reported to improve the octane number of the gasoline fuel as well (Patel and Singh 2014). Acetins could be produced by employing acetic acid (AcA) or acetic anhydride (AcAn) as acetylating agents for GL (Setyaningsih et al. 2018; Bedogni et al. 2017). Sandesh et al. (2015) and Han et al. (2019) reported that acetylation of GL with AcAn could be performed even at low reaction temperature of 30 °C; however, GL acetylation with AcA demands relatively higher temperature of up to 120 °C. Although AcAn-mediated GL acetylation demands milder reaction conditions, at the same time, it yielded AcA as a corrosive side product. Further, AcAn above 49 °C forms the explosive mixture with air, and hence, it is not considered suitable for the large-scale manufacturing of GT (Kong et al. 2016). On the other hand, utilization of AcA as acetylating agent would form harmless water as a side product. In the literature, GT has been primarily produced via homogeneous acid (H_2SO_4, H_3PO_4 or HCl)-catalysed GL acetylation with AcA or AcAn

✉ Amjad Ali
amjadali@thapar.edu

1 School of Chemistry and Biochemistry, Thapar Institute of Engineering and Technology, Patiala 147004, India

(Khayoon and Hameed 2011). Even the homogeneous catalyst-assisted and AcA-mediated acetylation demands higher temperature (up to 135 °C) and prolonged reaction duration (up to 3 h) to yield the partial GT selectivity (Khayoon and Hameed 2011). Moreover, such catalysts are not only toxic and corrosive but also non-reusable and difficult to separate from the reaction mixture. In order to circumvent the issues of homogeneous catalysts, GT production with AcA in the presence of acidic heterogeneous catalyst was been explored in the literature. The reactivity of the few literature-reported heterogeneous catalysts with that studied in the present work is compared in Table 1.

As evident from Table 1, most of the reported catalysts suffer the drawback of poor GT selectivity as well as poor reusability. These catalysts also required more than 100 °C reaction temperature to yield the acceptable conversion levels. However, the catalyst reported in the present study (SSZ-550) not only provides the excellent triacetin selectivity (93%) at 80 °C, but also able to demonstrate the reusability during 6 catalytic runs.

In order to impart the acidity to the heterogeneous catalysts, either Lewis acid sites (e.g. $M_2^{n+}O_n^{2-}$) or Brønsted acid sites (e.g. $-SO_3^-H^+$) have been introduced into the matrix. A variety of the heterogeneous acid catalysts such as metal oxide-based or sulphated one, viz. sulphated STA–ZrO$_2$–MCM-41 (Kaya Ekinci and Oktar 2019), Amberlyst (Kale et al. 2015; Rastegari et al. 2015), WO/TiO$_2$–ZrO$_2$, MoO$_3$/TiO$_2$–ZrO$_2$ (Reddy et al. 2010,) MP(10)/SBA-15 (Trejda et al. 2012) and SO$_4^{2-}$/CeO$_2$–ZrO$_2$ (Reddy et al. 2012), have been explored for the GL acetylation. Heteropolyacids (HPAs) are also strong Brønsted acids and could catalyse a wide variety of reactions including glycerol acetylation (Bhorodwaj and Dutta 2011); nevertheless, they suffer the drawbacks of having the low surface area, low thermal stability and solubility in polar media. In order to immobilize the HPAs, they have been supported over the MCM-41 (e.g. HPAs/ZrO$_2$–MCM-41) to impart them large surface area, higher thermal stability and insolubility in reaction medium (Kaya Ekinci and Oktar 2019).

Along with the catalytic sites, GT selectivity was also found to be a function of reaction duration, reagent ratio and reaction temperature (Reddy et al. 2010). Hence, an optimal combination of all these parameters is essential to achieve the maximum selectivity of GT.

With an aim to develop the reusable heterogeneous catalyst for the GL acetylation with AcA, (Scheme 1) sulphate groups have been appended over the siliceous zirconia matrix, in present study. Further, the reaction conditions have been optimized to achieve the maximum GT selectivity during the acetylation reaction. The catalyst stability and reusability have been evaluated with the recovered catalyst, and the reason for the decline of the catalyst activity has also been investigated.

Experimental section

Materials and methods

Zirconium (IV) oxychloride octahydrate and tetraethoxysilane (TEOS 98%) were procured from Sigma-Aldrich (USA). Ammonia solution, sulphuric acid, acetic acid (99%) and glycerol (99%) used for the acetylation were obtained from Loba Chemie Ltd. (India).

Table 1 Comparison of acetylation activity of few literature-reported catalysts

Catalyst	Tem (°C)	AcA/GL	Time (h)	wt%*	GM%	GD%	GT%	GLC%	Catalyst reusability (# of cycles)	References
STA–ZrO$_2$–MCM-41	200	6:1	4	5	37	42	21	100	NR	Kaya Ekinci and Oktar (2019)
CS–H$_2$SO$_4$	80	6:1	24	–	25	15	4	97	4	Malaika and Kozłowski (2018)
SO$_3$H/G–C	100	8:1	2.5	5	–	–	100	100	10	Karnjanakom et al. (2018)
Amberlyst 15	105	6:1	10	5	–	12.3	83.9	100	2	Kale et al. (2015)
Amberlyst-70	105	6:1	10	5	2.5	51.7	45.8	100	3	Kale et al. (2015)
PAmberlyst-36	100	7:1	25	3	43	44	13	100	3	Rastegari et al. (2015)
MP(10)/SBA-15	150	9:1	NR	1.5	9	51	40	78	4	Trejda et al. (2012)
HSiW/ZrO$_2$	120	10:1	4	3	28.3	60.5	11.2	96.4	4	Zhu et al. (2013)
SO$_4^{2-}$/CeO$_2$–ZrO$_2$	120	6:1	1	5	25.8	57.7	16.5	100	5	Reddy et al. (2012)
PW2_AC	120	16:1	3	2	25	63	11	86	3	Ferreira et al. (2011)
WO/TiO$_2$–ZrO$_2$	120	6:1	3	5	53.21	40	6.78	99	NR	Reddy et al. (2010)
MoO$_3$/TiO$_2$–ZrO$_2$	120	6:1	3	5	52	40.45	7.52	100	5	Reddy et al. (2010)
SSZ-550	80	9:1	0.7	3	–	7	93	100	6	PR

*Catalyst wt% with respect to glycerol, *S* sulphonic acid-functionalized, *AC* activated carbon, *G–C* glycerol–carbon, *GL* glycerol, *GM* glycerol monoacetate, *GD* glycerol diacetate, *GT* glycerol triacetate, *GLC* glycerol conversion, *NR* not reported, *P* pressure (1 bar), *PR* present report
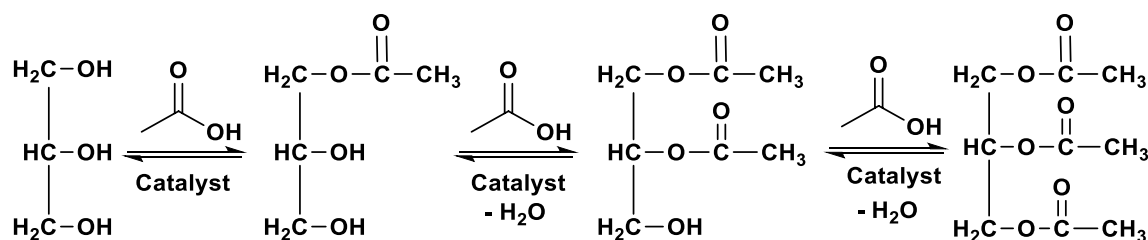
Scheme 1 Stepwise glycerol acetylation with acetic acid in the presence of catalyst

Powder X-ray diffraction data were collected by PANalytical X'Pert Pro using Cu-K$_a$ radiation (operated at 45 kV) in 2θ range of 20° to 70°. Fourier transform infrared spectra (FTIR) of samples were recorded in KBr matrix on Agilent Cary-660 spectrophotometer. Surface area was measured by Brunauer, Emmett and Teller (BET) method and pore size by BJH method using Micro Trac-BEL mini-II instrument. Prior to analysis, samples were heated at 100 °C for 3 h under vacuum to remove any adsorbed molecule from the catalyst surface. The sulphated siliceous zirconia (SSZ-550) surface acidity was calculated by conducting temperature-programmed desorption of NH$_3$ (NH$_3$-TPD) analysis using the Micro Trac-Belcat II instrument. The Brønsted and Lewis acidic sites of the catalyst were demonstrated by Pyridine adsorption method. Catalyst sample under investigation was initially saturated with pyridine, dried at 50 °C for 2 h, further heated for 10 min at 300 °C to desorb the pyridine and finally subjected to the diffuse reflectance FTIR analysis.

Scanning electron microscopy coupled with energy-dispersive X-ray spectrometry (SEM–EDX) was performed over JEOL JSM 6510LV instrument, and transmission electron microscope (TEM) images were recorded on Hitachi 7500 instruments. X-ray photoelectron spectra (XPS) were determined by ESCA + instrument (omicron nanotechnology, Oxford Instrument, Germany) equipped with monochromator aluminium source (Al K radiation of 1486.7 eV energy).

TA in the reaction mixture was detected and quantified by high-performance liquid chromatography (HPLC) which was performed over Agilent Infinity 1200 instrument. Prior to the analysis, catalyst from the reaction mixture was filtered out and the liquid phase, thus obtained, was dissolved in 60/40 (v/v) hexane/isopropanol (IPA) solvent system. A fixed sample volume of 20 μL was injected into the HPLC instrument which was analysed at 35 °C column temperature. During the analysis, 60/40 (v/v) hexane/IPA was employed as mobile phase with a flow rate of 0.6 mL/min and RX-SIL column (250 × 4.6 mm, 5 μm) as a stationary phase. The retention time of the molecules, present in the sample under investigation, was detected with the help of refractive index (RI) detector.

Preparation of siliceous zirconia

The Si(OH)$_4$Zr(OH)$_4$ matrix has been prepared by sol–gel method using ZrOCl$_2$·8H$_2$O as precursor of zirconia. In a representative preparation method, ZrOCl$_2$·8H$_2$O (5 g) was dissolved in 20 mL deionized water under constant stirring at room temperature (35 °C). To this, aqueous ammonia solution was added dropwise until 10 pH was obtained and the resulted mixture was stirred for 15 min. To this, tetraethoxysilane (TEOS, 98%) was added (corresponding to theoretical 1:1 molar ratio of Si/Zr) slowly, with constant stirring for 1 h at room temperature. Finally, the mixture was filtered and washed with deionised water multiple times to remove the chloride ions and then dried at 100 °C for 12 h to obtain the matrix Si(OH)$_4$Zr(OH)$_4$ which is referred as SZ.

To incorporate the sulphate ion over the matrix, 1 g of prepared matrix (SZ) was powdered and suspended in 20 mL deionized water. To this, 1 molar solution (3 mL) of H$_2$SO$_4$ was also added. The resulted mixture was stirred for 24 h at room temperature, then dried for 12 h at 100 °C and finally calcined at 550 °C for 4 h in a muffle furnace. The catalyst (referred as SSZ-550) preparation is shown in Scheme 2.

Acetylation of glycerol with acetic acid

The optimum reaction condition for the GL acetylation was established by varying the temperature (30–100 °C), AcA-to-GL molar ratio (3–12) and catalyst amount (1–5 wt% of GL). To evaluate the catalyst reusability, it was recovered from the reaction mixture by centrifugation, washed with methanol and calcined at 550 °C. The catalyst thus regenerated was employed in six successive cycles under the same experimental and regeneration conditions.

Scheme 2 Reaction scheme for the formation of sulphated siliceous zirconia (SSZ-550) catalyst
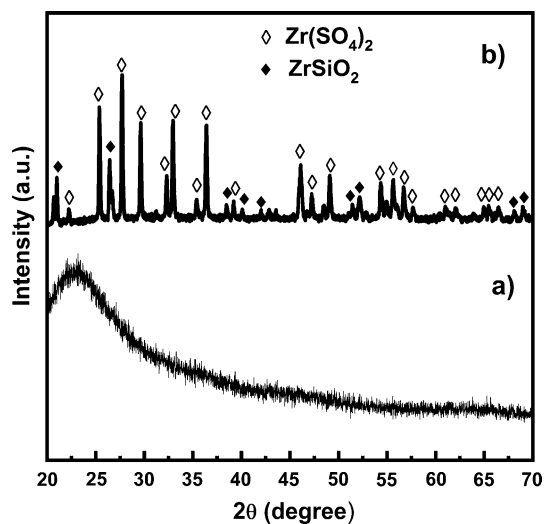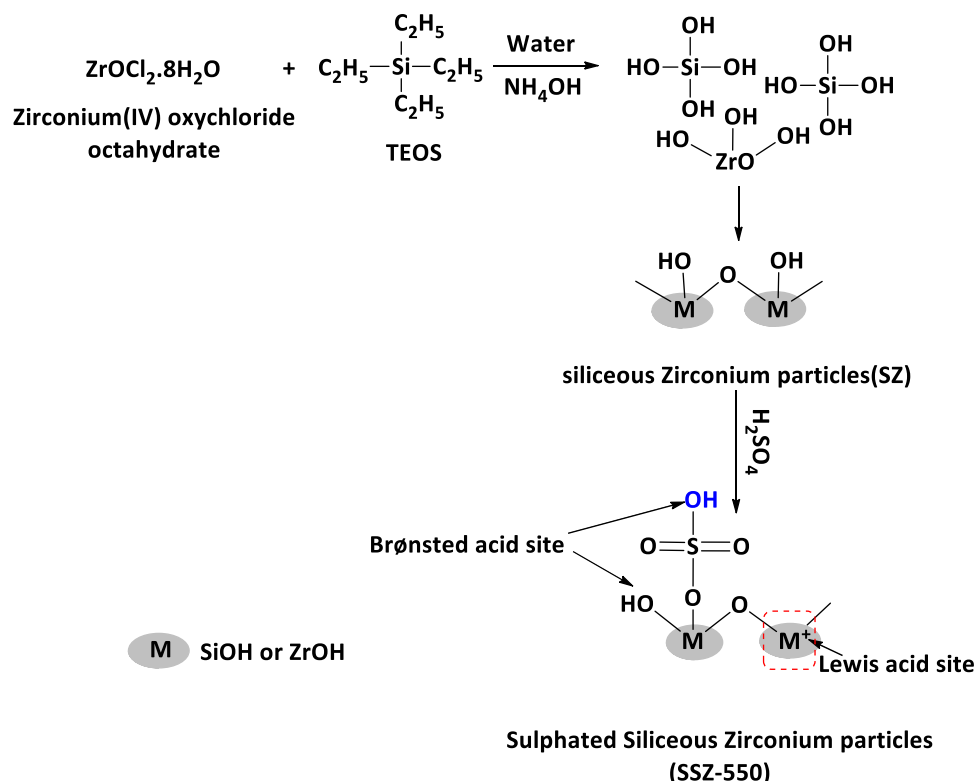

siliceous Zirconium particles(SZ)

Brønsted acid site

M SiOH or ZrOH

Lewis acid site

Sulphated Siliceous Zirconium particles (SSZ-550)

Fig. 1 Powder XRD spectra of the **a** SZ and **b** SSZ-550

Results and discussion

Catalyst characterization

XRD analysis

The X-ray diffraction (XRD) patterns for SZ demonstrate a broad hump ($2\theta = 22$), as shown in Fig. 1a, to support the amorphous nature of the prepared matrix. On incorporating the sulphate group over the matrix, SSZ-550 has been formed which was found to exist in crystalline phase as evident by the appearance of the sharp peaks in the XRD patterns (Fig. 1b). The crystalline nature of the material was due to the formation of $ZrSiO_2$ as minor phase (JCPDF = 01-081-0590) and $Zr(SO_4)_2$ as major phase (JCPDF = 00-024-1492), as shown in Fig. 1b. The crystallite size of the $Zr(SO_4)_2$ phase, calculated by the Scherrer equation, was found to be 13.2 nm.

FTIR spectroscopy analysis

The FTIR spectra of the prepared SZ and SSZ-550 are compared in Fig. 2 to indicate the sulphate group anchoring over the siliceous zirconia surface. Both the samples show a strong band at ~ 802 cm^{-1} due to the vibrations of Si–O–Si bond. In the literature, the presence of a band at 808 cm^{-1} in the FTIR spectra has been reported to indicate the presence of Si–O–Si bonding (Hu et al. 2013). In the FTIR spectra, new bands in the range of ~ 1028–1266 cm^{-1} were observed (Fig. 2b), due to the stretching vibrations corresponding to S–O and S=O bonds to support the incorporation of sulphate group over the siliceous zirconia matrix. Similar observation was reported by Sun and Garcia (Garcia et al. 2008; Sun et al. 2005) where the bands in the range of 1045–1223 cm^{-1} have been reported to indicate the anchoring of sulphate ion over the siliceous zirconia matrix.
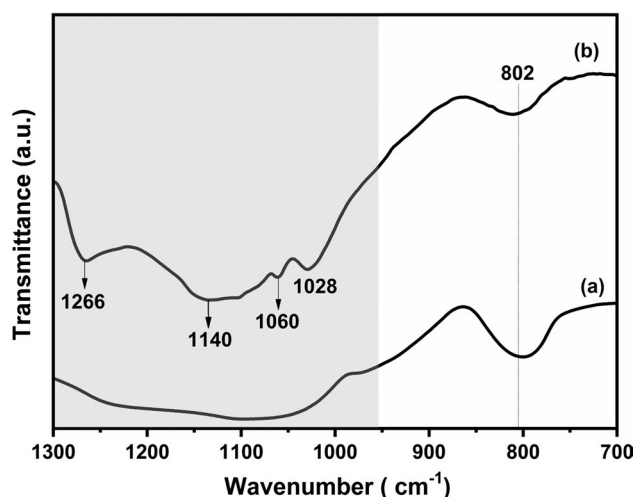
Fig. 2 FTIR spectra of the **a** SZ and **b** SSZ-550

BET analysis

The BET surface area of SZ and SSZ-550 was measured by N_2 adsorption desorption isotherms as represented in Fig. 3. All the samples were found to exhibit type IV curves of IUPAC classification, which indicates the mesoporous nature of the samples. In case of the siliceous zirconia (SZ), matrix surface area and pore volume were found to be 197.1 m^2 g^{-1} and 0.31 cm^3 g^{-1}, respectively, as shown in Fig. 3b. However, upon sulphate group impregnation over the SZ matrix, surface area (69.9 m^2 g^{-1}) as well as pore volume (0.10 cm^3 g^{-1}) was found to decrease. The drop in the surface area could be ascribed to the pore blockage of the matrix upon sulphate group attachment. Ward et al. also observed the reduction of surface area (from 709 to 342 m^2 g^{-1}) as well as pore volume (from 0.819 to 0.430 cm^2 g^{-1}) when sulphated zirconia was impregnated over the mesoporous silica surface (Ward et al. 2011).

NH$_3$ temperature-programmed desorption study

The acidic sites present over the catalyst surface were quantified by the temperature-programmed desorption of ammonia (NH_3-TPD). The TPD profiles of the desorbed NH_3 from SZ and SSZ-550 catalysts are shown in Fig. 4. A broad peak in the range of 233–243 °C, for both the samples, was observed owing to the ammonia desorption from weak acidic sites. However, sulphate incorporation over the siliceous zirconia nanoparticles demonstrates an additional desorption peak at 473 °C (4.96 mmol g^{-1}) to indicate the formation of strong acidic sites. Chen et al. (2007) have been reported that sulphated silica–zirconia (SiO_2–SZ) nanoparticles showed desorption peaks in the range of 210–290 °C and 460–600 °C to indicated the presence of weak and strong acidic sites, respectively, over the catalyst surface (Ganpat and Gbadebo 2013).

Pyridine adsorption study

To study the nature of the acidic sites present over the catalyst surface, pyridine-saturated matrix and catalyst were subjected to FTIR spectroscopy. Through this method, Brønsted and Lewis acid sites present over the catalyst could be identified and differentiated (Parry 1963). As shown in Fig. 5, the siliceous zirconia matrix shows a single band at 1636 cm^{-1} owing to the presence of Brønsted (B) acidic sites on its surface. Upon SO_4^{2-} incorporation over the SZ matrix, new bands at 1445, 1490, 1545 and 1613 cm^{-1} were observed in addition to the band observed in the matrix. Thus, incorporation of the sulphate group over the matrix leads to the formation of the Brønsted as well as Lewis acidic sites. The
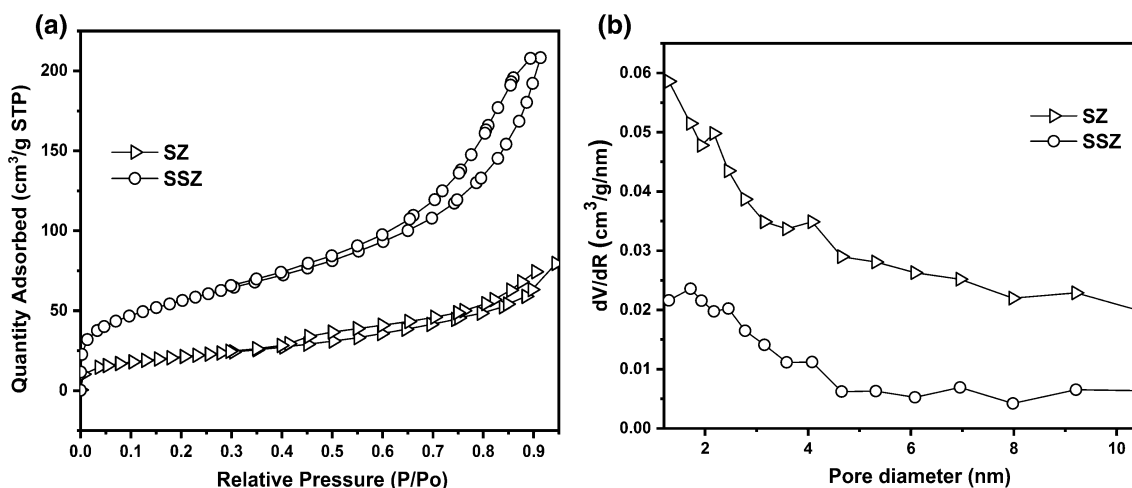

Fig. 3 **a** N_2 adsorption–desorption isotherms and **b** pore distribution branch of the nitrogen isotherm by the BJH
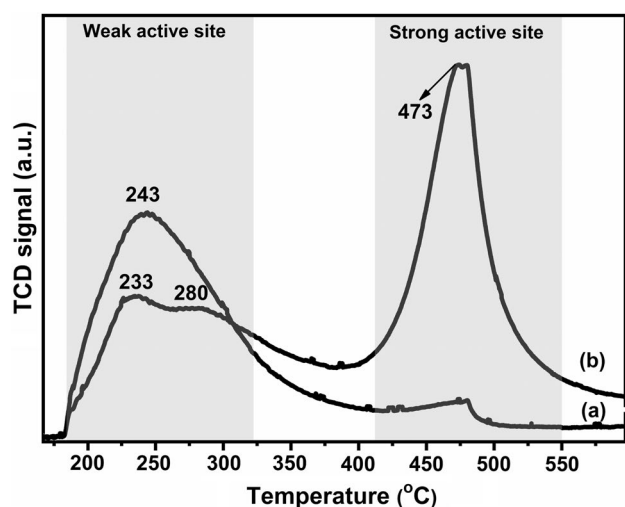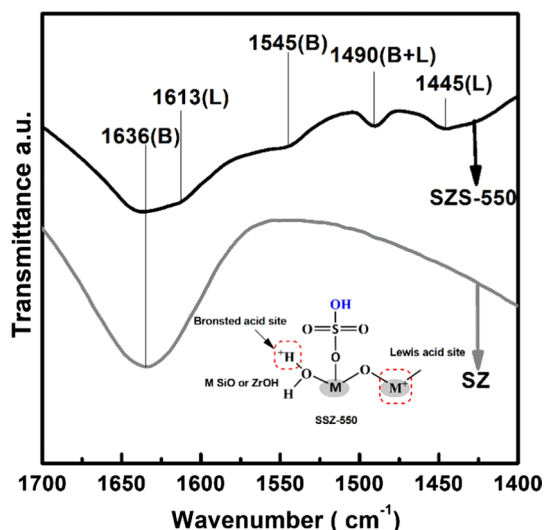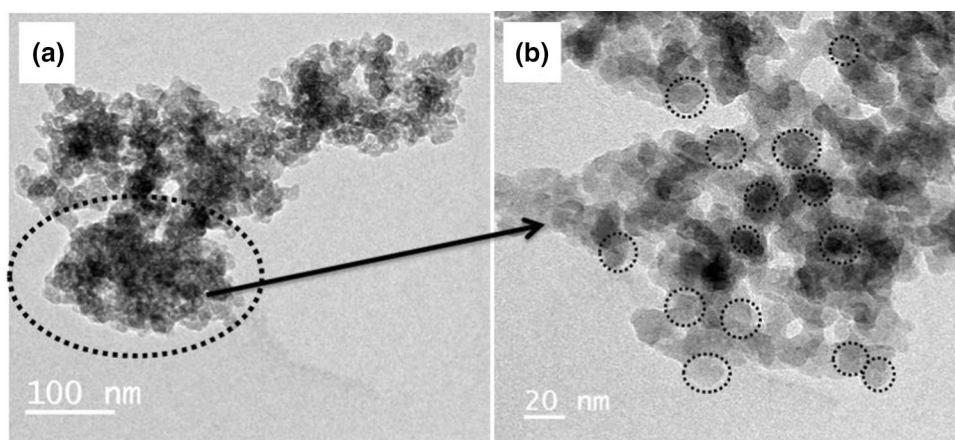
Fig. 4 Ammonia TPD analysis of **a** SZ and **b** SSZ-550

Fig. 5 FTIR spectra of pyridine-absorbed SZ and SSZ-550

Brønsted sites interacts with pyridine which leads to the formation of pyridinium ions, and same could be identified due to the presence of bands at 1490 and 1545 cm^{-1} in the FTIR spectrum. In the literature, similar bands were also reported at 1450, 1487 and 1540 cm^{-1}, to support the formation of pyridinium cations, owing to the interaction of pyridine with Brønsted acids (Kansedo and Lee 2012; Yang and Kou 2014; Massam and Brown 1995). Chomel et al. (2006) concluded that sulphate group is mainly responsible for the generation of strong acidic sites which impart the acetylation activity to the catalyst.

SEM, EDX, elements mapping and TEM analysis

The morphology and elemental distributions of the catalyst particles were examined by SEM–EDX technique, and corresponding elemental mapping is shown in Fig. ESM-1. The SEM images of the siliceous zirconia (Fig. ESM-1a) and sulphated siliceous zirconia (Fig. ESM-1b) show the formation of agglomerated nanoparticles in irregular geometries. Elemental mapping clearly demonstrates that all the elements (O, Si, Zr and S) are uniformly distributed over the catalyst surface.

TEM image of SSZ-550 was studied in order to get the information about the particle size and geometry as shown in Fig. 6. The TEM analysis of SSZ-550 revealed the formation of spherical agglomerated particles (~ 16 nm particles size), which is close to the crystallite size (15.2 nm) calculated from XRD data. The smaller particle size could be correlated with the higher catalyst surface exposure to the reactants which may facilitate the higher catalyst activity.

XPS study

The XPS spectra of silicon, sulphur, zirconia and oxygen are presented in Fig. 7 for determining the electronic state of the elements present in the catalyst. The band observed
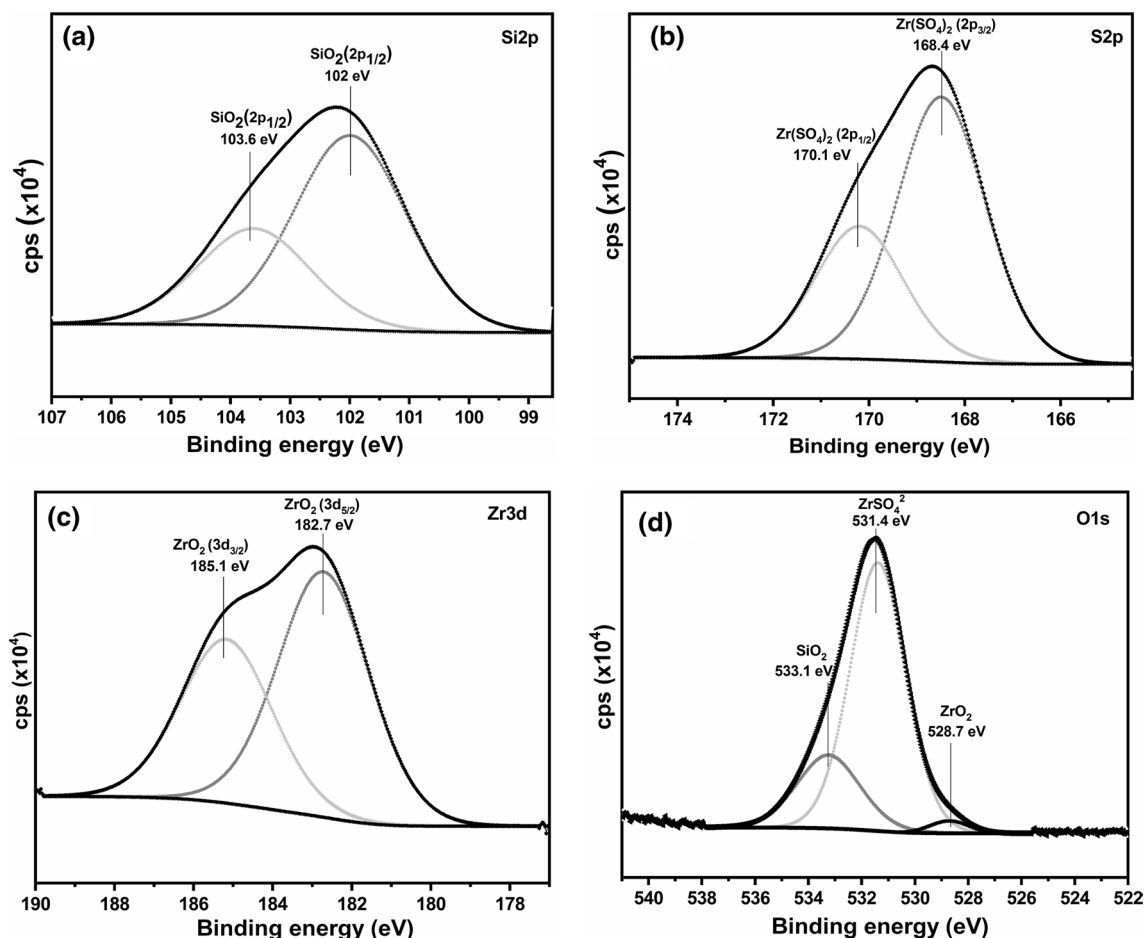
Fig. 6 TEM images of SSZ-550 **a** low and **b** high resolution

Fig. 7 XPS spectra of the various elements present in SSZ-550: **a** Si2*p*, **b** S2*p*, **c** Zr3*p* and **d** O1*s*

at 103.6 eV and 102 eV could be attributed to $2p_{1/2}$ and $2p_{3/2}$ level of Si^{4+} as shown in Fig. 7a. Observed values are very close to the literature-reported values of 103.1 eV and 102 eV for $Si^{4+}2p$ state present in SiO_2 material (Chernavskii et al. 2006; Malhotra and Ali 2019). The presence of sulphate functional group over the siliceous zirconia matrix could be attributed to the presence of two peaks at 168.4 and 170.1 eV corresponding to the $S^{+6}2p_{3/2}$ and $S^{+6}2p_{1/2}$ states, respectively (Fig. 7b). These binding energy values also support the linkages of sulphate group with zirconia/silica matrix as the reported binding energies for the sulphate group anchored over the ZrO_2 matrix were found to be at 168.9 and 169.2 eV (Hino et al. 2006). The XRD analysis of the same material also indicates the formation of $Zr(SO_4)_2$; however, owing to the amorphous nature of the silica, no peak due to the silica sulphate could have been observed. Anchoring of the sulphate group over the matrix was also supported by the FTIR analysis of the catalyst as discussed in earlier section. Furthermore, the XPS spectrum shows (Fig. 7c) peaks at 185.1 and 182.7 corresponding to the $Zr^{4+}3d_{3/2}$ and $Zr^{4+}3d_{5/2}$ states, respectively. This study

could be correlated with the literature, where the presence of Zr^{4+} has been ascribed to the appearance of peaks at 182.9 and 185.3 eV for $Zr^{4+}3d_{5/2}$ and $Zr^{4+}3d_{3/2}$ states, respectively, in ZrO_2 phase (Desmartin-Chomel et al. 2006). The peaks (Fig. 6d) at 528.7, 533.1 and 531.4 eV may be due to the presence of $O^{2-}1s$ state of lattice oxygen and could also be ascribed to the various linkages of oxygen present in the catalyst, viz. Si–O–Si, S–O–Zr and Zr–O–Si, respectively. Similar observations were reported in the literature, where the presence of $O^{2-}1s$ in the sulphated siliceous zirconia nanoparticles was supported by the presence of peaks at 532.4 and 532.5 eV corresponding to Si–O–Si or Zr–O–Si and S–O–Zr linkage (Rosenberg et al. 2002).

Product analysis

FTIR spectroscopy

Formation of the GT could be supported with the help of FTIR spectroscopic technique. In the FTIR spectra of glycerol, two bands at 1042 and 3300 cm^{-1} were observed due to

the C–O and O–H group stretching frequencies, respectively, as shown in Fig. ESM-2a. Upon glycerol acetylation, a new band at 1737 cm^{-1} (Fig. ESM-2b), due to –C=O group, was observed to support the formation of ester bond. The absence of any band in –OH region further supports the acetylation of all three glycerol hydroxyl groups.

HPLC analysis

The major product, GT, formed during the reaction was confirmed by comparing its retention time (6.30 min) with that of standard GT sample, as shown in the HPLC chromatogram in Fig. ESM-3. The HPLC chromatogram (Fig. ESM-3c) of product shows no peak corresponding to the glycerol (8.90 min) to confirm its 100% conversion into the product molecules. The quantitative analysis of the product mixture further supports the GT selectivity of 93% while remaining 7% being the glycerol diacetate (GD).

Catalyst screening

Prior to the catalyst screening, in blank runs, acetylation of GL with AcA was performed in the absence of catalyst, or in the presence of bare siliceous zirconia matrix. It is evident from Fig. ESM-4 that in the absence of catalyst merely 11.5% GL conversion with negligible GT selectivity was obtained, while the matrix material, bare siliceous zirconia, was able to yield 69% GL conversion with 1.6% GT selectivity. Thus, sulphate group anchoring over the matrix is required to generate the acidic sites which is primarily responsible for catalysing the glycerol acetylation. Reddy et al. (Trejda et al. 2012) also suggested that sulphate-impregnated CeO$_2$–ZrO$_2$ and CeO$_2$–Al$_2$O$_3$ catalysts demonstrate better GT selectivity (90%) at 120 °C reaction temperature, while carrying out the reaction at 6:1 AcA-to-GL molar ratio and in the presence of 5 wt% of catalyst amount.

In order to demonstrate the effect of reaction parameters on the catalyst activity, in the present study, the reagent ratio, catalyst amount, reaction temperature and reaction time have been sequentially varied as discussed in subsequent section.

Effect of AcA/GL molar ratio on product selectivity

Conversion of GL as well as GT selectivity over SSZ-550 at 80 °C on 3 wt% of catalyst (with respect to GL) with varying AcA/GL molar ratio (from 3 to 12) is shown in Fig. 8a. Theoretically, every molecule of GL required three molecules of AcA to achieve the 100% TA selectivity. However, to push the equilibrium in the forward direction, the reaction is usually performed in the presence of excess amount of AcA. During the present study, the use of lower AcA/GL molar ratio (up to 3) was found to yield a mixture of products which is dominated by the GM (41%),

GD (34%), GT (12%) and unreacted GL. On increasing the molar ratio up to 9, GT yield was found to increase up to 93% within 40 min of reaction duration. In the literature, at 3:1 AcA/GL molar ratio, SO$_4^{2-}$/CeO$_2$–ZrO$_2$ catalyst was found to demonstrate the poor GT selectivity of 5% along with GM yield of 25%. Even on increasing the molar ratio up to 6, the GT selectivity was found to increase marginally (from 5 to 16%) that too at higher reaction temperature of 120 °C and after a prolonged duration of 3 h (Trejda et al. 2012).

Effect of catalyst amount on product selectivity

In order to optimize the catalyst amount, acetylation of GL was studied in the presence of SSZ-550 catalyst using AcA as acetylating agent. Upon acetylation of GL with AcA (9:1 molar ratio) in the presence of 1–5 wt% catalyst (with respect to GL) at 80 °C, the selectivity of GT significantly increases due to the gradual increase in the active sites in the reaction mixture. It can be seen that at lower catalyst amount (up to 2 wt%), 90% GL conversion was observed but yielding the lower glycerol triacetate selectivity (46%) along with the formation of some GM (14%) and GD (30%) by-products. Maximum GT selectivity of 93% was obtained, at the cost of GM and GD, when 3 wt% of catalyst was employed, and a further increase in catalyst amount (up to 5 wt%) was neither found to improve the selectivity not able to reduce the reaction duration (Fig. 8b).

The same phenomenon is also reported in the literature for the acetylation of GL with AcA (1:7 molar ratio) at 100 °C reaction temperature in the presence of acidic catalyst (Lewatit catalyst), where an increase in catalyst amount from 2 to 3 wt% was also found to improve the GT selectivity from 56.28 to 66.91% (Setyaningsih et al. 2018).

Effect of reaction temperature on product selectivity

Acetylation of GL in the literature has been reported to follow the endothermic pathway and hence, external source of heat is essential to push the reaction in the forward direction (Patel and Singh 2014). In order to study the effect of temperature on GL conversion as well as product selectivity, a series of reaction was performed in the presence of SSZ-550 catalyst by varying the temperature in the range of 30 to 100 °C, as shown in Fig. 8c. A significant increase in GT selectivity from 0 to 93% was observed when the reaction temperature was raised from 30 to 80 °C, respectively. A further increase in the reaction temperature was not resulted in any significant increase in GT selectivity. Hence, reaction should be performed at 80 °C to achieve the optimum catalyst activity.
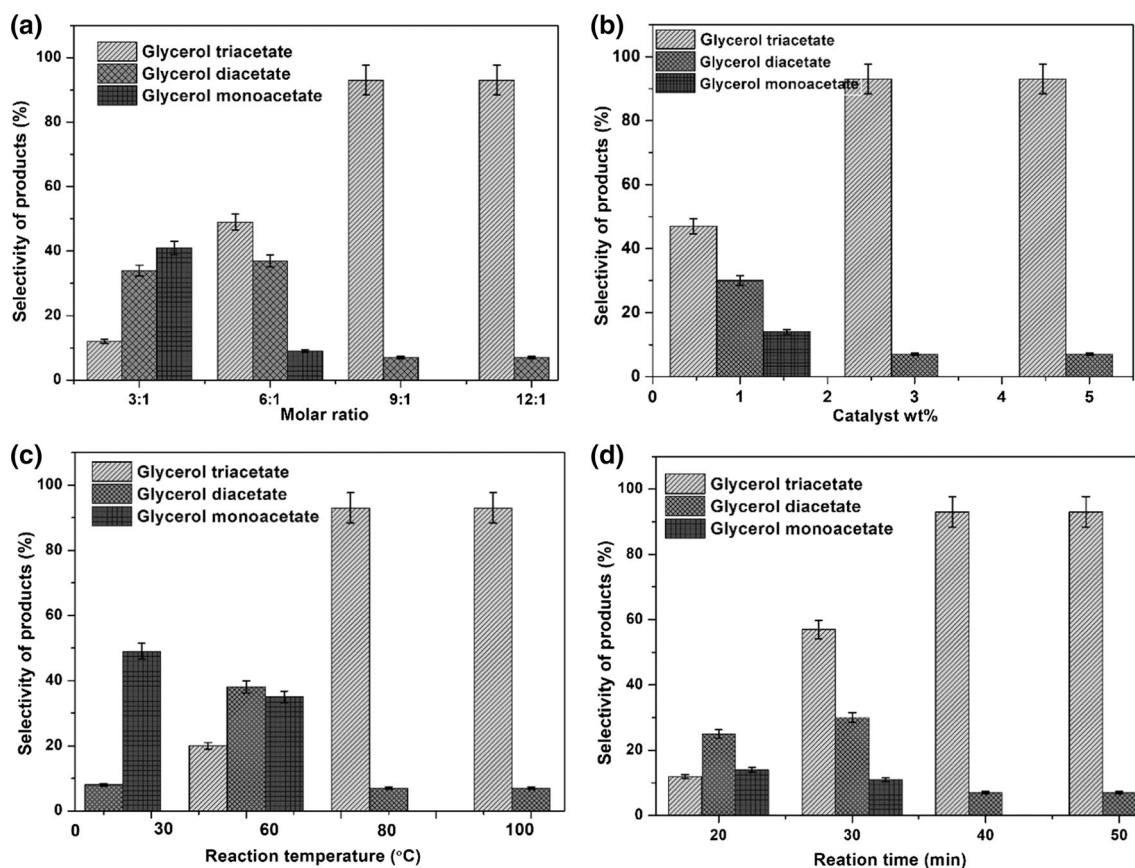
Fig. 8 Influence of the **a** molar ratio of AcA to GL [reaction conditions: reaction time = 40 min, catalyst amount = 3 wt% (with respect to GL) and reaction temperature = 80 °C], **b** catalyst amount with respect to GL (reaction conditions: AcA/GL = 9:1 molar ratio, reaction time = 40 min and reaction temperature = 80 °C), **c** reaction temperature [reaction conditions: AcA/GL = 9:1 molar ratio, reac-

tion time = 40 min and catalyst amount = 3 wt% (with respect to GL)] and **d** reaction time, on the products selectivity during GL acetylation [reaction conditions: AcA/GL = 9:1 molar ratio, catalyst amount = 3 wt% (with respect to GL) and reaction temperature = 80 °C]

Effect of reaction time on product selectivity

To establish the reaction duration in order to achieve the maximum GT selectivity, a series of GL acetylation was performed at 80 °C in the presence of 3 wt% catalyst at constant AcA/GL molar ratio of 9:1 (Fig. 8d). It is evident from the plot that during first 20 min of reaction period GD (25%) is the leading product and remains predominant till 30 min of reaction duration. However, after 40 min, GT became the exclusive product (93%) to support that GL acetylation took place in a step wise fashion. Reddy et al. (Trejda et al. 2012) have also studied the extent of GL acetylation at various time intervals over SO_4^{2-}/CeO_2–ZrO_2 catalyst at 120 °C and observed 63% and 11% selectivity of GD and GT, respectively, within 0.5 h of reaction duration in the presence of 6:1 AcA/GL molar ratio. Same study reported a maximum GT selectivity of 90%, nevertheless after prolonged reaction duration of 4 h. Thus, our study as well as literature report

supported the stepwise acetylation of GL and an increase in GT selectivity on increasing the reaction duration.

The reusability and stability

The reusability of SSZ-550 catalyst was evaluated under the optimized reaction conditions, viz. AcA/GL molar ratio of 9:1, 3 wt% of catalyst (with respect to GL), 80 °C reaction temperature and 40 min of reaction duration. As shown in Fig. 9, the SSZ-550 catalyst was employed during six catalytic runs under the identical reaction conditions and after every run the catalyst was recovered from the mixture through filtration washed with methanol to remove the reactants/products from the catalyst surface, dried at 100 °C for 12 h and finally calcined at 550 °C for 4 h. The results revealed that during first 3 catalytic cycles up to 80% GT selectivity which was found to decline gradually to 54% in 6th cycle.
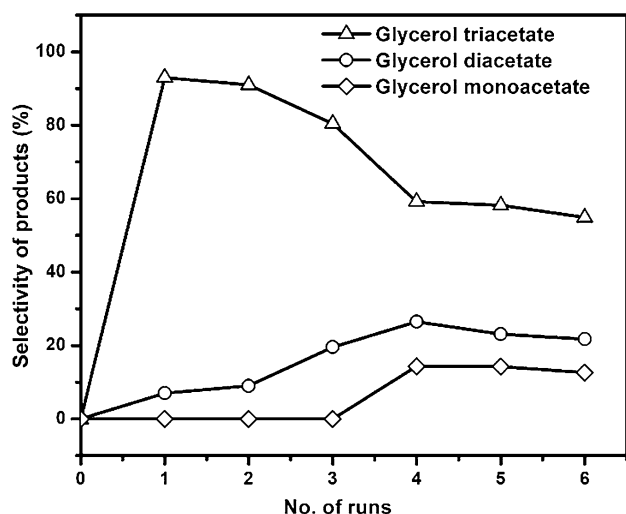
Fig. 9 Study of the SSZ-550 reusability during the GL acetylation with AcA. Reaction conditions: AcA/GL = 9:1 molar ratio, reaction time = 40 min, catalyst amount = 3 wt% (with respect to GL) and reaction temperature = 80 °C

In order to establish the reason(s) behind the loss in catalytic activity, NH$_3$-TPD profile of fresh and reused catalysts is compared in Fig. 10a. Fresh catalyst exhibited the strong acid sites, as revealed from the desorption peak at 473 °C, with total acidity of 4.96 mmol g^{-1} in comparison with 1.36 mmol g^{-1} for the spent catalyst at the same desorption temperature. Thus, a decrease in catalyst acidity could be attributed to loss of acidic strength which might be due to the loss of sulphate species from the catalyst surface.

In order to evaluate the loss of sulphate ions from the catalyst surface, the FTIR spectra of fresh and spent catalyst are compared in Fig. 10b. The partial loss of the SO$_4^{2-}$ moiety from the spent catalyst is evident due to the loss of bands at 1028, 1140 and 1266 cm^{-1}. The absence of any vibrational

band associated with the TG or GL in the FTIR of reused catalyst further maintained that organic molecules have not collected over the catalyst facade to hinder the active sites.

As evident from the FTIR study, sulphate group has been detached from the catalyst surface during the repeated use. The leached active sites from the matrix may catalyse the reaction similar to the homogeneous catalyst. In order to quantify the homogeneous contribution in the catalyst activity, a hot filtration test was performed. During the test, acetylation of GL was performed under optimized reaction parameters for 20 min and after that catalyst was separated from the reaction mixture with the help of simple filtration. Now, the reaction mixture, without catalyst, was allowed to react for additional 20 min. As evident from Fig. 11, no significant change in the GL conversion level was observed when the reaction was allowed to continue in the absence of catalyst. Thus, it is safe to assume that dissolved catalyst contents, if any, were not able to catalyse the reaction to significant extent and heterogeneous catalyst is primarily responsible for almost entire catalytic activity.

Proposed mechanism for the acetylation of GL with acetic acid

As indicated by the blank experiments ("Catalyst screening" section) in the absence of catalyst, merely 11.5% GL conversion with negligible GT selectivity was obtained. On the other hand, bare siliceous zirconia was able to yield merely 1.6% GT selectivity with higher GL conversion level of 69%. These experiments clearly indicate the catalytic role of strong Brønsted acid cites (SO$_4^-$H$^+$) during the synthesis of GT. However, relatively higher GL conversion levels were obtained with bare catalyst, due to the presence of surface Brønsted acidic sites (O$^-$H$^+$) (structure I in scheme 3); nevertheless, these sites are not strong enough to yield the higher GT selectivity. Sulphate group anchoring over the
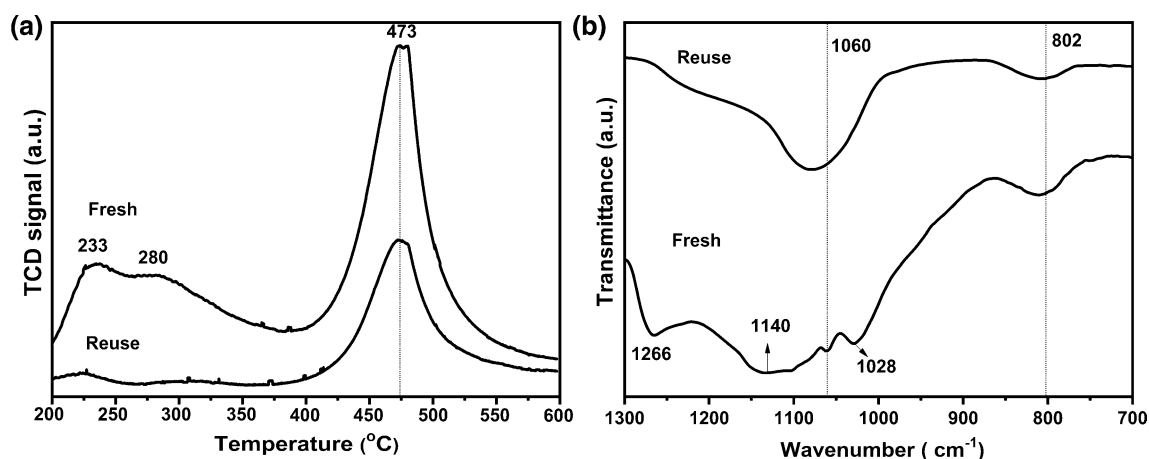

Fig. 10 Comparison of **a** TPD and **b** FTIR plot of fresh and reused catalyst
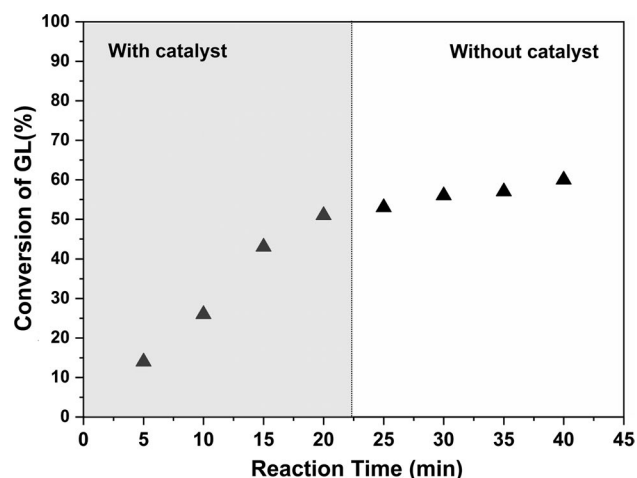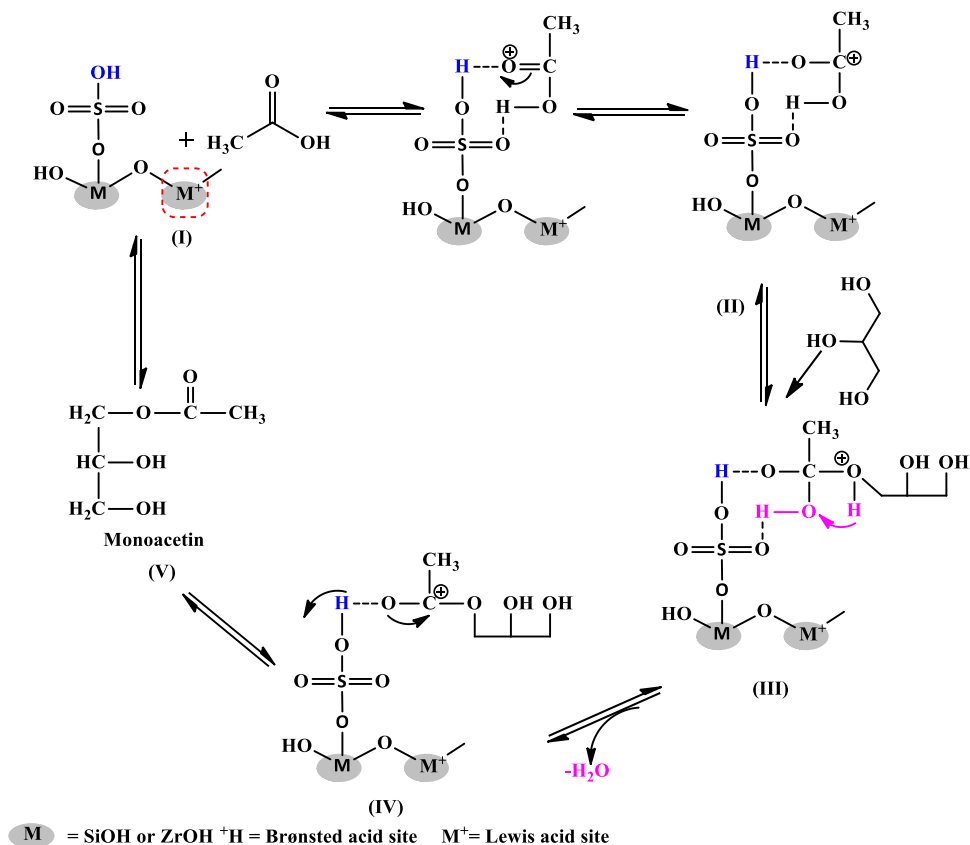
Fig. 11 Homogeneous contribution analysis during the GL acetylation (catalyst amount—3 wt%, AcA/GL molar ratio—9:1, reaction temperature 80 °C)

siliceous zirconia matrix imparted the strong Brønsted acidity, and consequently, the SSZ-550 catalyst was able to yield 93% GT selectivity with overall 100% GL conversion within 40 min of reaction duration. Homogeneous sulphuric acid has also been reported to catalyse the acetylation of mono- as well tri-alcohol (GL) and found to follow the (pseudo)

first-order kinetic model (Setyaningsih et al. 2018; Zhou et al. 2012). Consequently, in the present study, sulphate groups have been proposed as the reaction centres for initiating the GT synthesis.

As discussed earlier ("Effect of reaction time on product selectivity" section), the GM selectivity was found to be maximum in the beginning of the reaction which gradually got converted into the GD and GT to support the stepwise acetylation of the GL. During the present study ("Effect of AcA/GL molar ratio on product selectivity" section), when the AcA concentration was varied, the rate of GT formation was also found to change. However, same was not found to be effected when GL concentration was varied.

Thus, plausible mechanism assumes the sulphate group-assisted protonation of the acetic acid carbonyl group in the first step of the reaction to form the carbocation (II) as an intermediate (Kale et al. 2015; Zhou et al. 2012; Venkatesha et al. 2016) as shown in Scheme 3. Now the carbocation (II) may react with the –O–H of GL to form another intermediate (III). A water molecule has been given away by the intermediate (III) to generate a new carbocation (IV). Carbocation (IV) ultimately regenerates the catalyst and leads to the formation of the GM (V). Now, one of the remaining two –OH groups of GM would further react with AcA following the similar mechanism as described above to form GD which may further react with AcA to form the GT molecule.

Scheme 3 Proposed mechanism of glycerol acetylation with acetic acid in the presence of SSZ-550 catalyst

Conclusion

Glycerol acetylation with acetic acid was performed in the presence of the SSZ-550 heterogeneous acid catalyst to yield the 93% glycerol triacetate during a quick succession of 40 min. The presence of Brønsted acidic sites, in the form of sulphate group, was found to be accountable for the higher catalytic activity. The catalyst was recovered from the reaction mixture and reused during six catalytic runs albeit, with partial loss in activity owing to the fractional loss of sulphate group from the catalyst surface. Such a high glycerol triacetate yield under ambient reaction conditions in the presence of reusable heterogeneous catalyst has not been frequently reported in the literature. Presently the work is in progress, in our laboratory, to improve the catalyst stability in order to achieve the better catalyst reusability.

Compliance with ethical standards

Conflict of interest The authors declare that there is no conflict of interest.

References

Bedogni GA, Acevedo MD, Aguzín F, Okulik NB, Padró CL (2017) Synthesis of bioadditives of fuels from biodiesel-derived glycerol by esterification with acetic acid on solid catalysts. Environ Technol 39(15):1955–1966. https://doi.org/10.1080/09593330.2017.1345986

Bhorodwaj SK, Dutta DK (2011) Activated clay supported heteropoly acid catalysts for esterification of acetic acid with butanol. Appl Clay Sci 53:347–352. https://doi.org/10.1016/j.clay.2011.01.019

Chen X, Ju Y, Mou C (2007) Direct synthesis of mesoporous sulfated silica-zirconia catalysts with high catalytic activity for biodiesel via esterification. J Phys Chem C 111(50):18731–18737. https://doi.org/10.1021/jp0749221

Chernavskii PA, Khodakov AY, Pankina GV (2006) In situ characterization of the genesis of cobalt metal particles in silica-supported Fischer–Tropsch catalysts using Foner magnetic method. Appl Catal A Gen 306:108–119. https://doi.org/10.1016/j.apcata.2006.03.033

Desmartin-Chomel A, Flores JL, Bourane A, Clacens JM, Figueras F, Delahay G, Giroir Fendler A, Lehaut-Burnouf C (2006) Calorimetric and FTIR study of the acid properties of sulfated titanias. J Phys Chem B 110:858–863. https://doi.org/10.1021/jp0530698

Edward M, Peter O, Hilary R (2014) The use of impregnated perlite as a heterogeneous catalyst for biodiesel production from marula oil. Chem Pap 68(10):1341–1349. https://doi.org/10.2478/s11696-014-0583-1

FAO, OECD (2015) OECD-FAO agricultural outlook 2015–2024. OECD, Paris. https://doi.org/10.1787/agr_outlook-2015-en

Ferreira P, Fonseca IM, Ramos AM, Vital J, Castanheiro JE (2011) Acetylation of glycerol over heteropolyacids supported on activated carbon. Catal Commun 12:573–576. https://doi.org/10.1016/j.catcom.2010.11.022

Fregolente PBL, Pinto GMF, Wolf-Maciel MR, Filho RMI (2010) Monoglyceride and diglyceride production through lipase-catalyzed glycerolysis and molecular distillation. Appl Biochem Biotechnol 160:1879–1887. https://doi.org/10.1007/s12010-009-8822-6

Ganpat V, Gbadebo Y (2013) Mesoporous nanocrystalline sulfated zirconia synthesis and its application for FFA esterification in oils. Appl Catal A Gen 463:196–206. https://doi.org/10.1016/j.apcata.2013.05.005

Garcia CM, Teixeira S, Marciniuk LL, Schuchardt U (2008) Transesterification of soybean oil catalyzed by sulfated zirconia. Bioresour Technol 99:6608–6613. https://doi.org/10.1016/j.biortech.2007.09.092

Goscianska J, Malaika A (2019) A facile post-synthetic modification of ordered mesoporous carbon to get efficient catalysts for the formation of acetins. Catal Today. https://doi.org/10.1016/j.cattod.2019.02.049

Han X, Zhu X, Ding Y, Miao Y, Wang K, Zhang H, Wang Y, Liu S (2019) Selective catalytic synthesis of glycerol monolaurate over silica gel-based sulfonic acid functionalized ionic liquid catalysts. Chem Eng J 359:733–745. https://doi.org/10.1016/j.cej.2018.11.169

Hino H, Kurashige M, Matsuhashi H, Arata K (2006) The surface structure of sulfated zirconia: studies of XPS and thermal analysis. Thermochim Acta 441:35–41. https://doi.org/10.1016/j.tca.2005.11.042

Hu X, Hao X, Wu Y, Zhang J, Zhang X, Wang PC, Zou G, Liang XJ (2013) Multifunctional hybrid silica nanoparticles for controlled doxorubicin loading and release with thermal and pH dual response. J Mater Chem B 1:1109–1118. https://doi.org/10.1039/c2tb00223j

Jiahui Z, Yuanfeng W, Xianghai S, Siquan X, Shuai L, Yanli Z, Lijing G, Jin Z, Guomin X (2018) Thermodynamic and kinetic studies for synthesis of glycerol carbonate from glycerol and diethyl carbonate over Ce–NiO catalyst. Chem Pap 72(11):2909–2919. https://doi.org/10.1007/s11696-018-0518-3

Kale S, Umbarkar SB, Dongare MK, Eckelt R, Armbruster U, Martin A (2015) Selective formation of triacetin by glycerol acetylation using acidicion-exchange resins as catalyst and toluene as an entrainer. Appl Catal A Gen 490:10–16. https://doi.org/10.1016/j.apcata.2014.10.059

Kansedo J, Lee KT (2012) Transesterification of palm oil and crude sea mango (*Cerbera odollam*) oil: the active role of simplified sulfated zirconia catalyst. Biomass Bioenergy 40:96–104. https://doi.org/10.1016/j.jcat.2017.08.001

Karnjanakom S, Maneechakr P, Samart C, Guan D (2018) Ultrasound-assisted acetylation of glycerol for triacetin production over green catalyst: a liquid biofuel candidate. Energy Convers Manag 173:262–270. https://doi.org/10.1016/j.enconman.2018.07.086

Kaya Ekinci E, Oktar N (2019) Production of value-added chemicals from esterification of waste glycerol over MCM-41 supported catalysts. Green Process Synth 8:128–134. https://doi.org/10.1515/gps-2018-0034

Khadijeh BG, Nilofar A, Mohd AY, Mohd WS (2014) Mesoporous phosphated and sulphated silica as solid acid catalysts for glycerol acetylation. Chem Pap 68(9):1194–1204. https://doi.org/10.2478/s11696-014-0550-x

Khayoon MS, Hameed BH (2011) Acetylation of glycerol to biofuel additives over sulfated activated carbon catalyst. Bioresour Technol 102:9229–9235. https://doi.org/10.1016/j.biortech.2011.07.035

Kong PS, Aroua MK, Wan Daud WMA, Lee HV, Cognet P, Pérès Y (2016) Catalytic role of solid acid catalysts in glycerol acetylation for the production of bio-additives: a review. RSC Adv 6:68885–68905. https://doi.org/10.1039/c6ra10686b

Malaika A, Kozłowski M (2018) Glycerol conversion towards valuable fuel blending compounds with the assistance of SO$_3$H-functionalized carbon xerogels and spheres. Fuel Process Technol 184:19–26. https://doi.org/10.1016/j.fuproc.2018.11.006

Malhotra R, Ali A (2019) 5-Na/ZnO doped mesoporous silica as reusable solid catalyst for biodiesel production via transesterification of virgin cottonseed oil. Renew Energy 133:606–619. https://doi.org/10.1016/j.renene.2018.10.055

Massam J, Brown DR (1995) The roles of Bronsted and Lewis surface acid sites in acid-treated montmorillonite supported ZnC$_{12}$ alkylation catalysts. Catal Lett 35:335–343. https://doi.org/10.1007/bf00807190

Parry EP (1963) An infrared study of pyridine adsorbed on acidic solids. Characterization of surface acidity. J Catal 2:371–379. https://doi.org/10.1016/0021-9517(63)90102-7

Patel A, Singh S (2014) A green and sustainable approach for esterification of glycerol using 12-tungstophosphoric acid anchored to different supports: kinetics and effect of support. Fuel 118:358–364. https://doi.org/10.1016/j.fuel.2013.11.005

Rastegari H, Ghaziaskar HS, Yalpani M (2015) Valorization of biodiesel derived glycerol to acetins by continuous esterification in acetic acid: focusing on high selectivity to diacetin and triacetin with no byproducts. Ind Eng Chem Res 54:3279–3284. https://doi.org/10.1021/acs.iecr.5b00234

Reddy PS, Sudarsanam P, Raju G, Reddy BM (2010) Synthesis of bio-additives: acetylation of glycerol over zirconia-based solid acid catalysts. Catal Commun 11:1224–1228. https://doi.org/10.1016/j.catcom.2010.07.006

Reddy PS, Sudarsanam P, Raju G, Reddy BM (2012) Selective acetylation of glycerol over CeO$_2$–M and SO$_4^{2-}$/CeO$_2$–M (M=ZrO$_2$ and Al$_2$O$_3$) catalysts for synthesis of bioadditives. J Ind Eng Chem 18:648–654. https://doi.org/10.1016/j.jiec.2011.11.063

Rosenberg DJ, Coloma F, Anderson JA (2002) Modification of the acid properties of silica-zirconia aerogels by in situ and ex situ sulfation. J Catal 228:218–228. https://doi.org/10.1006/jcat.2002.3656

Sandesh S, Manjunathan P, Halgeri AB, Shanbhag GV (2015) Glycerol acetins: fuel additive synthesis by acetylation and esterification of glycerol using cesium phosphotungstate catalyst. RSC Adv 5:104354–104362. https://doi.org/10.1039/c5ra17623a

Setyaningsih L, Siddiq F, Pramezy A (2018) Esterification of glycerol with acetic acid over Lewatit catalyst. MATEC Web Conf 154:01028. https://doi.org/10.1051/matecconf/201815401028

Sun Y, Ma S, Du Y, Yuan L, Wang S, Yang J (2005) Solvent-free preparation of nanosized sulfated zirconia with Brønsted acidic sites from a simple calcination. J Phys Chem B 109:2567–2572. https://doi.org/10.1021/jp046335a

Trejda M, Stawicka K, Dubinska A, Ziolek M (2012) Development of niobium containing acidic catalysts for glycerol esterification. Catal Today 187:129–134. https://doi.org/10.1016/j.cattod.2011.10.033

Venkatesha NJ, Bhat YS, Prakash BSJ (2016) Volume accessibility of acid sites in modified montmorillonite and triacetin selectivity in acetylation of glycerol. RSC Adv 10:45819–45828. https://doi.org/10.1039/c6ra05720a

Ward AJ, Pujari AA, Costanzo A, Masters AF, Maschmeyer T (2011) Ionic liquid-templated preparation of mesoporous silica embedded with nanocrystalline sulfated zirconia. Nanoscale Res Lett 6:192. https://doi.org/10.1186/1556-276X-6-192

Yang Y, Kou Y (2014) Determination of the Lewis acidity of ionic liquids by means of an IR spectroscopic probe. Chem Commun. https://doi.org/10.1039/b311615h

Zhou L, Nguyen T, Adesina A (2012) The acetylation of glycerol over amberlyst-15: kinetic and product distribution. Fuel Process Technol 104:310–318. https://doi.org/10.1016/j.fuproc.2012.06.001

Zhu S, Zhu Y, Gao X, Moa T, Zhu Y, Li Y (2013) Production of bio-additives from glycerol esterification over zirconia supported heteropolyacids. Bioresour Technol 130:45–51. https://doi.org/10.1016/j.biortech.2012.12.011